MEASUREMENTS OF ENERGY, ENERGY SPREAD AND BUNCH WIDTH AT THE UNILAC

J. Klabunde, V. Schaa, E. Schaffner, P. Strehl, H. Vilhjalmsson, D. Wilms
GSI, Gesellschaft für Schwerionenforschung mbH
Darmstadt, Fed. Rep. of Germany

Summary

Characteristics of various beam diagnostic elements, including computation of signal shapes and signal processing, will be discussed. Some procedures for determination of beam parameters in longitudinal phase space are presented. Instrumentation and the computer program of a self-contained on-line energy measurement will be described.

Introduction

At the UNILAC, frequent changes of accelerating conditions (various ions, various energies between 3.6 - 10 MeV/u, use of foil or gas stripper) and demands for perfect beam quality (required micro-structure of bunches and pure energy spectrum on target) are standard. For efficient tuning of all rf substructures involved in accelerating processes, a rather elaborated diagnostic system for measurement of beam parameters in longitudinal phase space is essential.

A short description of fast pick-up probes and a survey of a temporary signal processing system used in commissioning of the UNILAC is given in Ref. 1. Experience from routine operation in recent years, and study periods for accelerator development, led to improvement of signal processing and utilization of measurements of longitudinal phase space.

In the present paper, various methods of measurement and signal evaluation are described in more detail. On the basis of some typical examples, the capability of procedures for efficient tuning of a multiparticle, variable-energy machine will a multistage rf accelerating system will be demonstrated.

Characteristics of Diagnostic Elements and Measurement Procedures

To measure beam parameters in longitudinal phase space, the following types of probes are in use at the UNILAC:

- broad band coaxial Faraday cups
- semiconductor detectors
- broad band capacitive pick-ups.

Figure 1 gives a schematic layout of the UNILAC and the experimental areas. The various elements produce signals with different characteristics, which will be described below.

Coaxial Faraday cup

Design details (without pneumatic actuator for positioning the device into beam) are shown in Fig. 2. The cup was designed to have a 50-ohm geometry. The reflection coefficient measured by a TDR (25-ps rise time test pulse) is less than 5%. A grid in front of the collector plate (not shown in Fig. 2) repels secondary electrons and shields against the longitudinal electrical field moving in front of the bunch. Both effects would result in a broadening of the fast current signals, as illustrated in Fig. 3.

The influence of longitudinal electrical fields on signal shape can be estimated for simple bunch geometries. The true induced current is given by:

$$i = \frac{d}{dt} \int_0^R \varepsilon_0 E_Z 2\pi r dr \qquad (1)$$

where R = radius of collector plate placed at Z=0 and E_Z = longitudinal electrical field of the moving bunch. Assuming a bunch of lengthΔ t, with uniform charge distribution over time t, and neglecting field distortions by the cup itself, the result is (NR-approximation):

$$\frac{i}{N\zeta} = \frac{e}{2\Delta t}\left(\frac{\beta c(t+\Delta t/2)}{\sqrt{(\beta c(t+\Delta t/2))^2+R^2}} - \frac{\beta c(t-\Delta t/2)}{\sqrt{(\beta c(t-\Delta t/2))^2+R^2}}\right), \qquad (2)$$

where N = number of ions within the bunch and ζ = charge state of ions. The sum of the induced current according to (2) and pure charge current leads to a signal shape as shown in Fig. 4.

Coaxial Faraday cups are used for bunch length measurements, bunch shape observation and optimization, determination of correct rf phase settings, and calculation of proper rf amplitudes for generating a good micro-structure.

Semiconductor detectors

Due to increased demands in the quality of the energy spectra at the end of UNILAC, and the frequently desired well-defined structure of bunches on target, semiconductor detectors (ORTEC: TF-40-400-60-S; SCHLUMBERGER: BTC-50-150-859) were installed. Detectors are mounted on compressed air actuated feed-throughs, and can be moved rapidly into the beam. A system of beam degraders for fixed and variable attenuation of beam intensity, protects the semiconductors. Movement of the degraders is controlled by an interlock system.

One of the detectors at the end of the UNILAC is placed in an approximately 1200-mm long diagnostic chamber, and can be mvoed 1000 mm along the beam axis with better than 1-mm precision. Therefore, time-of-flight measurements for energy determination are possible using this detector.

Depending on beam parameters to be measured, different preamplifiers were developed at GSI:

- charge sensitive preamplifiers (slow output) for measurement of energy spectra, with a gain of 1 - 20 mV/MeV and a bandwidth of about 70 MHz;
- voltage sensitive amplifiers (fast output) with a gain of 44 - 2200 mV/MeV and a bandwidth of about 450 MHz ($t_r \leq 1$ ns).

Signal processing following the preamplifiers utilized procedures common to nuclear and high energy physics.

At the UNILAC, semiconductor detectors are preferred for the measurement of energy spectra. Bunch length and energy determination are performed much more efficiently by using capacitive pick-ups. Figure 5 illustrates the capability of semiconductors for optimization of energy spectra.

The energy resolution of semiconductor detectors depends mainly on the energy and mass of the ions to be detected. For $^{84}Kr^{12+}$-ions, the resolution could be determined at W = 1.4 MeV/u to $\Delta W/W = (0.7 \pm 0.1)\%$, taking advantage of the small energy spread of the Wideröe prestripper accelerator, which was measured to $\Delta W_o/W_o = (0.08 \pm 0.02)\%$ with capacitive pick-ups.

For observation of time spectra, semiconductor signals, amplified by voltage sensitive preamplifiers, are processed in the well-known start-stop mode, using fast time-to-amplitude converters and a 4096-channel analyzer. Figure 6 shows a typical time spectrum of the bunches, where time calibration was made by subdividing the rf reference stop-signal. Using more advanced techniques, time resolution can be improved to 50 - 80 ps/channel, as shown for example, in Ref. 2.

Capacitive pick-ups

Probe Optimization and Signal Computation

Most efficient measurements in longitudinal phase space (see Ref. 2 for details) are done by using a system of capacitive pick-ups. Taking advantage of an elaborate program for computation of pick-up signals including probe and bunch parameters, the geometric shape of pick-ups could be optimized. Some insights into signal processing and signal interpretation could be gained. Relevant design parameters are shown in Fig. 7. Impedance was approximately calculated taking advantage of analogies between coaxial structure, as shown in Fig. 7, and a planar microstrip. Final matching to exactly 50 ohm is done by the bending of segmented diaphragms in front and behind the pick-up cylinder. In the case of precise matching, the reflection coefficient will be less than 5% for a test pulse with 25-ps rise time.

Shape and amplitudes of pick-up signals can be calculated to a good approximation under the following assumptions: A bunch with homogeneous charge distribution is moving with $v = \beta c$. The bunch has no dimensions in transverse directions Y and X. At time t, the center of charge is at a distance of $Z = \beta ct$ from the origin of the coordinate system at Z=0. For such a bunch, with $\Delta Z = \beta c \Delta t$, the charge distribution can be described by:

$$\rho(X,Y,Z) = \delta(X)\delta(Y)\frac{N\zeta e}{\beta c \Delta t}\,(\Theta(t+\Delta t/2)-\Theta(t-\Delta t/2)), \quad (3)$$

where $\delta(X)$ and $\delta(Y)$ are the well-known Dirac delta-functions and $\Theta(t)$ is the step function of Heaviside. Neglecting again distortions of potentials by the beam pipe and pick-up probe itself, the extracted signal current can be written (NR-approximation):

$$i(t) = \frac{N\zeta e}{2\Delta t}\left(\frac{L-\beta c(t+\Delta t/2)}{\sqrt{(L-\beta c(t+\Delta t/2))^2+R^2}} + \frac{\beta c(t+\Delta t/2)}{\sqrt{(\beta c(t+\Delta t/2))^2+R^2}}\right.$$
$$\left. - \frac{L-\beta c(t-\Delta t/2)}{\sqrt{(L-\beta c(t-\Delta t/2))^2+R^2}} - \frac{\beta c(t-\Delta t/2)}{\sqrt{(\beta c(t-\Delta t/2))^2+R^2}}\right), \quad (4)$$

where L, R and probe lengths and radius, respectively. In the chosen coordinate system, the probe is positioned from Z=0 to Z=L. Figure 8 shows some computed signals, assuming typical UNILAC β and Δt-values. For comparison in Fig. 8, one plot was calculated for a more realistic triangular shape charge distribution over the bunch, defining Δt by full-width half-maximum points.

Measured signal shapes agree very well with computation. Due to some uncertainties in signal amplification factors, cable dispersion, and plasma oscillations in the Penning source, it is very difficult, even within a 10% margin, to compare measured signal amplitudes with computed values. If strong plasma oscillations occur, as shown in Fig. 9, a comparison is impossible.

At the UNILAC, measurements of micro-structure with capacitive pick-ups, however, are the only possibility to detect such plasma oscillations. Experience has shown that optimization of a ion source by observing only the pick-up signals can be very efficient in terms of beam intensities. In some accelerator experiments, there was also observed an influence of plasma oscillations on beam quality at the end of UNILAC. This effect will be studied in more detail.

Signal Processing

Taking advantage of experience with the old temporary system as described in Ref. 1, some improvements and modifications on the signal processing system were implemented in recent years. As shown in Fig. 10, this results in a micro-

processor controlled pick-up signal selection, including some fixed programmed options (for example, automatic signal selection for energy measurements). The electronic system has been extended to also enable an on-line computed energy measurement. The capability of a new electronic system for fast determination of rf phases (also shown in Fig. 10) will be discussed in Ref. 2.

For signal amplification, a special broad-band amplifier with the following characteristics was developed at GSI:

Type	: Avantek UTO 1511, UTO 1521
Input impedance	: 50 ohm
Output impedance	: 50 ohm
Bandwith	: 5 - 1500 MHz
Gain	: 44 dB
Required input voltage for S:N=1:1	: $\sim$ 40 µV

Determination of Bunch Length

Measurements in the time domain

Due to convolution of the moving electrical bunchfield with the probe geometry, it is impossible to extract the bunch length directly from the observed probe signal. However, using Eq. 4, a relation between measured time, distance from positive-signal-maximum to negative-signal-minimum, Δk and bunch length Δt, can be derived. This relation is shown in Fig. 11. The procedure is mainly limited by the finite bandwidth of the 500-MHz oscilloscope used. For UNILAC beam parameters and capacitive pick-ups with L = 1 cm and R = 1.75 cm, the relation $\Delta k(\lim \Delta t \to 0) \sim 2L/\beta c$ also holds.

Measurement in the frequency domain

For values of Δt smaller than $\sim$ 0.8 ns, determination of bunch length, Δt, from an analysis of probe signal Fourier spectra is more effective. Using the program FAST FOURIER TRANSFORM (FFT), computation of such spectra for i(t) according to Eq. 4 and also for triangular shaped charge distribution of the bunches is straightforward. Approximating a typical pick-up signal by a polynominal relates the first minimum in the Fourier spectrum (harmonic number n), the period of accelerating rf (T) and bunch length Δt:

$$n_o = \frac{T}{\Delta t} \qquad (5)$$

This simple relation was confirmed also by FFT. Accuracy of this procedure gets better for small Δt, because from Eq. 5 it follows that

$$\delta(\Delta t) = - \left(\frac{T}{n_o^2}\right) \cdot \Delta n_o \qquad (6)$$

To estimate the bunch lengths Δt and compare different bunches with respect to signal rise time, observations in the frequency domain are very sensitive. Figure 12 demonstrates this clearly.

On-line energy measurement

A description of operator-aided procedure was given in Ref. 1. The new self-contained on-line procedure is illustrated in Fig. 13. For a single-valued plain determination of particle energy, the signals of probes T1, T2, T3, T4 (see Fig. 1) are used. Probe signals are sequentially switched by a computer controlled device to a selective rf amplifier, and tuned to the third harmonic of the bunch repetition frequency ($\triangleq$ 81 MHz). This harmonic was chosen because SN ratio is up to a factor of 40 better than with 27 or even 54 MHz. Bunch uncertainty can be eliminated by analyzing the phase relation of all 4 probe signals.

The 81-MHz signal is fed to a sampler. A 27-MHz reference signal of the phase axis is tripled in frequency and fed to a second sampler. Both samplers are controlled by a modified Hp-Vectrovoltmeter, which is synchronized by a 108-MHz reference signal from the poststripper accelerator phase axis. This procedure results in two 15-kHz sine wave signals on the sampler outputs, which are controlled in amplitude by a standard operational amplifier. Both sine wave signals are digitized by two synchronized fast CAMAC-ADC's (conversion rate 5 MHz, memory size 1000 points, corresponding to three 15-kHz periods). Digital data from all 4 probes and 27-MHz phase axis are evaluated in a PDP 11/34 by determination of the function

$$f_k(t) = A_k \sin(\omega t + \Psi_k) \qquad (7)$$

using a simple least squares fit. In Eq. 7, index k represents signal number (T1 - T4, phase axis), and A_k, Ψ_k are amplitude and phase of the fitted sine wave, respectively. Since the 27-MHz phase axis serves as time reference, Ψ_k=0 holds for this signal. From computed differences between Ψ_k-values corresponding to the probe signals, time-of-flight, and therefore also particle energy can be determined very precisely. Beam parameters available by evaluating A_k are not interpreted at present.

Based on good experiences with this on-line measurement, some more sophisticated, microprocessor-aided procedures of beam parameter control in longitudinal phase space will be implemented in the near future (see Ref. 2).

References

1 J. Glatz et al., Some Aspects of the Unilac Beam Diagnostic System, 1976 Proton Linear Accelerator Conference, Chalk River, AECC-5677.

2 L. Dahl et al., Longitudinal and Transverse Beam Optimization, these proceedings.

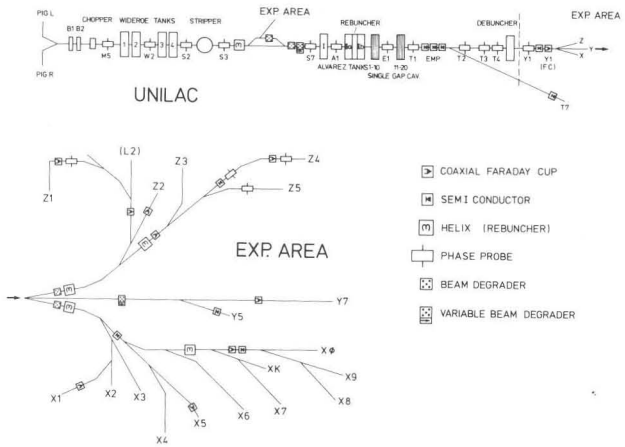

Fig. 1 Arrangement of beam diagnostic elements for measurements in longitudinal phase space along the UNILAC facility.

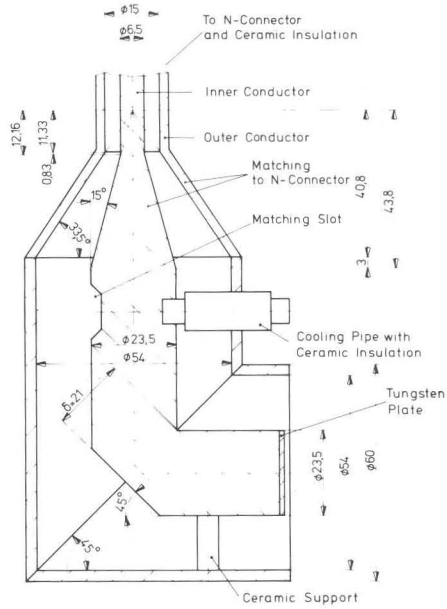

Fig. 2 Design of coaxial Faraday cup (dimensions in mm)

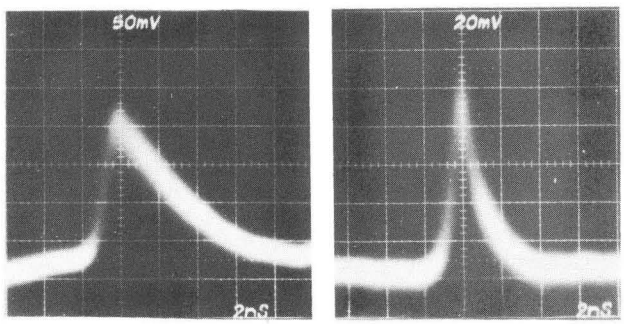

Fig. 3 Effect of secondary electrons and subsequent signal suppression by means of a grid in front of the collector plate. Left: without voltage on grid, Right: - 800 volts on grid, (mean beam current about 15 nA).

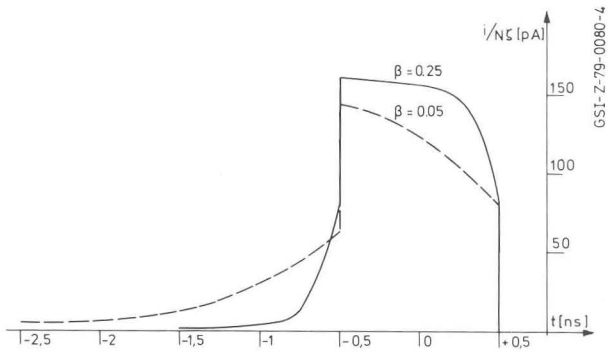

Fig. 4 Approximation of the effect of precursor longitudinal electrical field on signal shape observed by a coaxial Faraday cup.

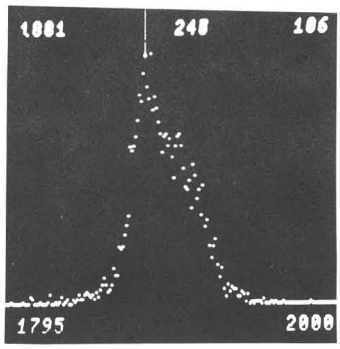

Incorrect setting of AI - Tank amplitude (FWHM ≃ 1.8 %).

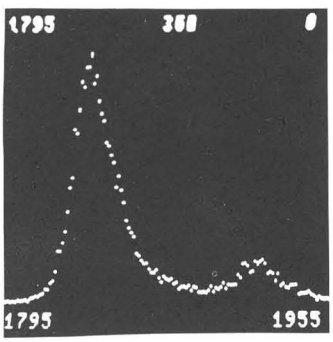

Incorrect bunch input phase (error about 500 ps, FWHM main peak on left: 1.2 %. Distance of satellite peak to main peak: ≃ 132 keV/u).

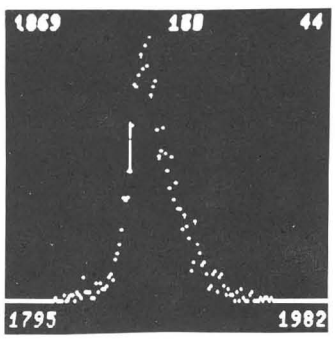

Correct settings (FWHM ≃ 1.1 %).

Fig. 5 Optimization of bunch input phase, rf amplitude setting for Alvarez I and rebuncher helix rf settings by observation of semiconductor energy spectra. Particle energy about 3.6 MeV/u, resolution (2 keV/u)/channel.

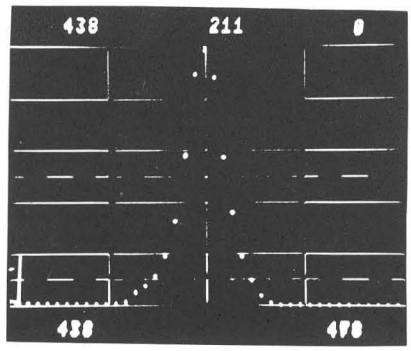

Fig. 6 Time spectra of bunches observed with a semiconductor detector behind a drift space.

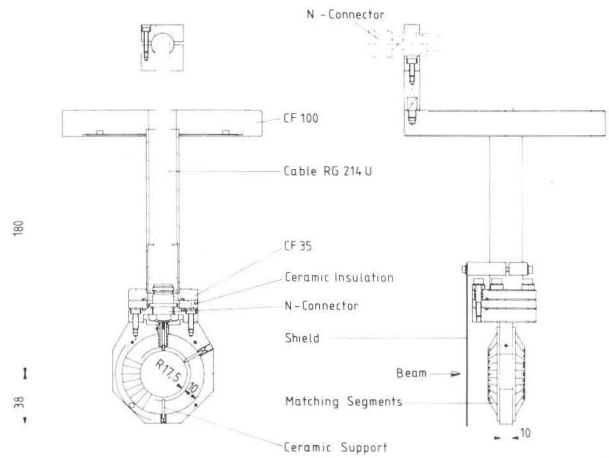

Fig. 7 Design of capacitive pick-up probes (dimensions in mm).

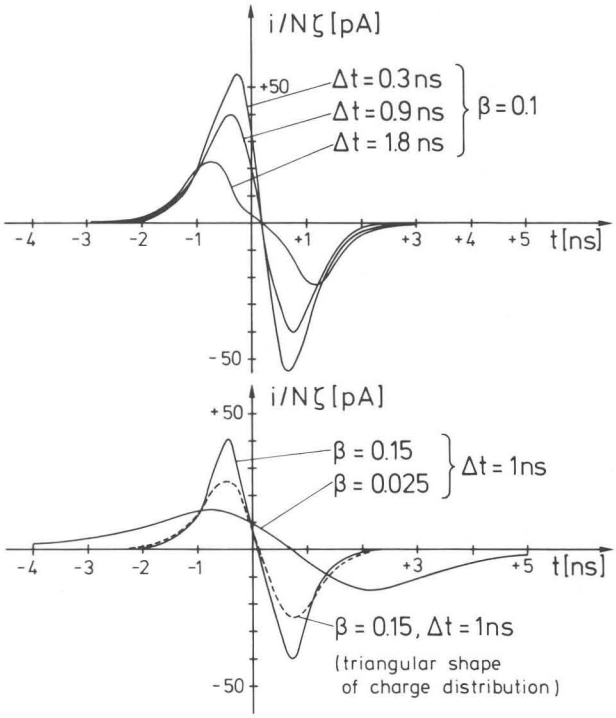

Fig. 8 Computed signal shapes for capacitive pick-ups using Eq. 4 and dimensions given in Fig. 7.

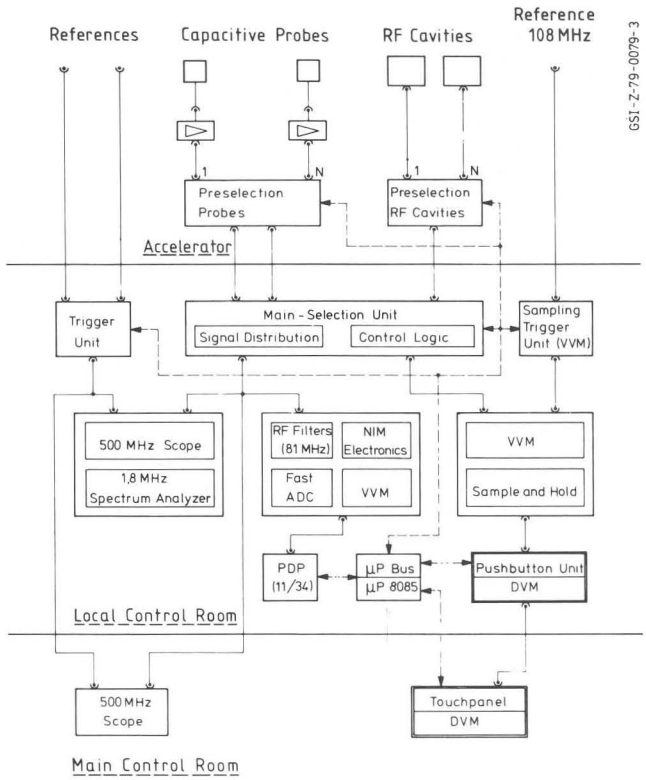

Fig. 10 Improved signal processing system for capacitive pick-ups and fast rf phase measurements.

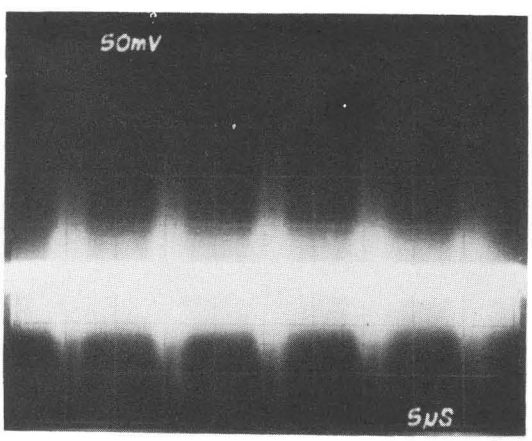

Fig. 9 Detection of ion-source plasma oscillations by means of capacitive pick-ups. In the time scale chosen, single beam bunches ($\Delta t \simeq 1.5$ ns) are not resolved. The lengths of the corresponding macro-pulse was 5 ms.

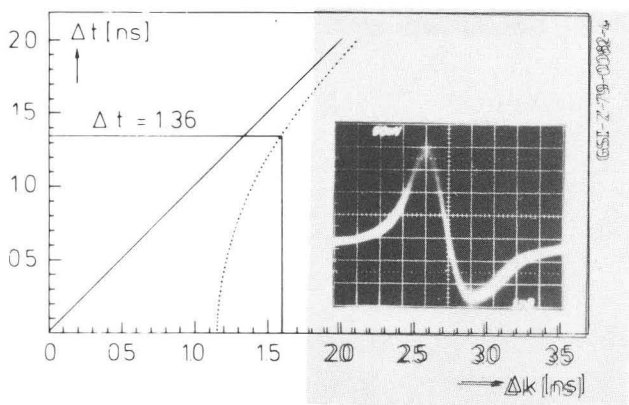

Fig. 11 Computed relation between bunch length Δt and measured time (Δk). Due to cable dispersion-effects, Δk should be determined as two times distance between maximum and zero crossing. Insert on right side shows the corresponding oscilloscope signal.

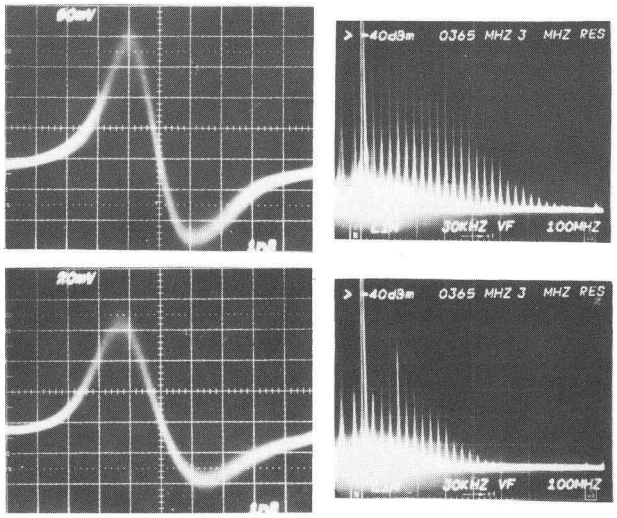

Fig. 12 Comparison of bunch signal observation in time and frequency domain, respectively (β ≃ 0.055).
Top left: Δk = 1.6 ns, Δt ≃ 1.36 ns (see Fig. 11)
top right: n_o ≃ 26, Δt ≃ 1.42 ns (see eq. (5))
bottom left: Δk = 2.0 ns, Δt ≃ 1.88 ns
bottom right: n_o ≃ 19, Δt ≃ 1.95 ns.

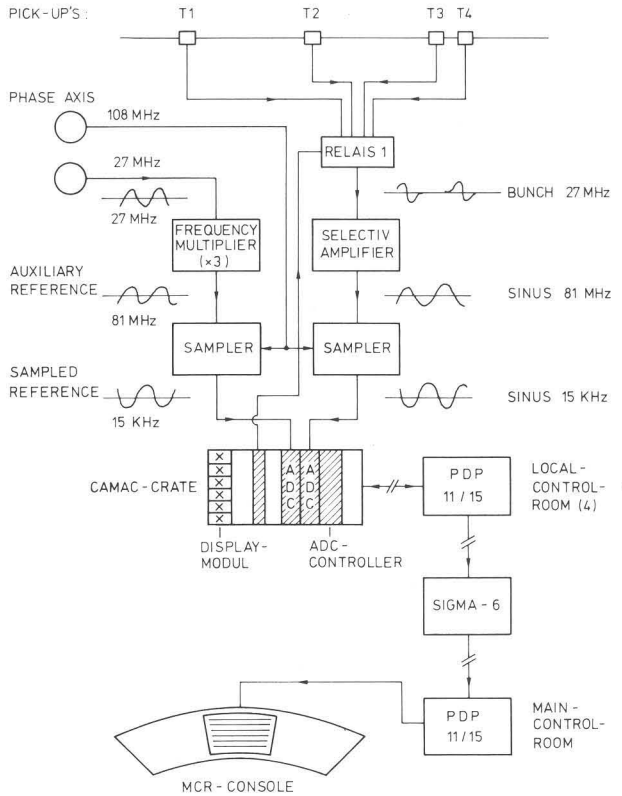

Fig. 13 Schematic block diagram of on-line energy measurement at UNILAC.